ChemComm

Multi-Principal Element Transition Metal Dichalcogenides via Reactive Fusion of Stochastic 3D - Heterostructures

Journal:	*ChemComm*
Manuscript ID	CC-COM-08-2018-006766.R2
Article Type:	Communication

Journal Name

COMMUNICATION

Multi-Principal Element Transition Metal Dichalcogenides via Reactive Fusion of 3D-Heterostructures

Received 00th January 20xx,
Accepted 00th January 20xx

DOI: 10.1039/x0xx00000x

www.rsc.org/

Ihor Z. Hlova,[a] Oleksandr Dolotko,[a] Brett W. Boote,[ab] Arjun K. Pathak,[a] Emily A. Smith,[a,b] Vitalij K. Pecharsky,[a,c] Viktor P. Balema[a]*

Transition metal dichalcogenides combining multiple principal elements in their structures are synthesized via mechanochemical exfoliation and spontaneous reassembly of binary precursors into 3D-heterostructures that are converted in single-phase layered materials by high-temperature reactive fusion. Physical and chemical events enabling these transformations are summarized in the form of conceivable reaction mechanism.

Layered transition metal dichalcogenides (TMDCs), with a general chemical formula of MX_2, where M is a group 4-6 refractory metal and X is S, Se, or Te, attract considerable attention as sources of single-layer nanomaterials for a broad range of applications.[1] Similar to graphite, bulk TMDCs are built from covalently bonded layers held together by weak van der Waals (vdW) forces (Fig. S1, ESI†). As a result, they can be exfoliated into nanosheets[2] each made up of metal atoms sandwiched between two parallel layers of chalcogens. Single-layer (2D) TMDCs show physical and mechanical properties similar to those of graphene but, in contrast to high electrical conductivity of the latter, 2D-TMDCs are tunable direct bandgap semiconductors.[3] The individual MX_2 nanosheets can serve as unique building blocks for 3D-heterostructures with exceptional quantum behaviours inaccessible with conventional materials.[4] Availability of compositionally diverse TMDCs is, therefore, critical for designing novel complex architectures for advanced applications.[1,5]

Binary TMDCs are fairly common. At the same time, the preparation of single-phase multi-principal element compounds remains challenging. Conventional alloying of two or more binary TMDCs could potentially enable the preparation of compositionally diverse hetero-element materials. However, an earlier attempt to synthesize a mixed single-phase $(Mo_{0.5}W_{0.5})S_2$ from bulk MoS_2 and WS_2 was unsuccessful[6] and, to the best of our knowledge, synthesis of single-phase multi-principal element TMDCs from binary MX_2 precursors has not been reported in the literature.

On several occasions, minuscule quantities of few-element TMDCs were synthesized using elaborate experimental techniques, with chemical vapour deposition (CVD) emerging as the most popular approach.[1] Based on gas-phase reactions between volatile metal precursors and vaporized S, Se, Te, or organic chalcogenides,[7] CVD becomes prohibitively expensive if more than mg-scale quantities of TMDCs are desired. Therefore, the latter are often prepared by reacting elemental metals with sulphur or selenium,[1,6] or via thermal decomposition of co-crystallized metal salts, such as $(NH_4)_2MoS_4$ and $(NH_4)_2WS_4$, in a reducing atmosphere.[3,8] Both methods find limited use owing to poor availability of starting ammonium salts, mass transfer and phase-segregation issues.

Herein, we describe a versatile synthetic approach enabling simple and reliable preparation of potentially unlimited array of single-phase multi-principal element TMDCs, and reveal the underlying mechanism of their formation. It appears that this practically unknown class of metal chalcogenides may be related to actively researched high-entropy alloy families. [9] It is worth noting that multi-principal element materials, such as high-entropy metal alloys, often show an improved thermodynamic stability due to high configurational entropy contribution to their Gibbs free energy of formation. A similar stabilization might also be expected both for bulk (3D) multi-element TMDCs and their 2D-derivatives. Finally, we also show that mechanochemical method can be adapted to the generation of 3D-heterostructures, thus opening doors to a variety of novel functional nanomaterials.

Initially, we explored mechanochemical technique as conceivable way of synthesizing mixed single-phase TMDCs from binary precursors because it often allows to produce homogeneous alloys and compounds from poorly miscible or thermolabile materials, whose direct alloying is impossible to achieve otherwise.[10] An equimolar mixture of commercially available MoS_2 and WS_2 was ball-milled under argon in a Fritsch Pulverisette 7 planetary mill at 600 rpm until Bragg

[a] *Ames Laboratory of U.S. Department of Energy, Iowa State University, Ames, IA, 50011-2416, E-mail: vbalema@ameslab.gov*
[b] *Department of Chemistry, Iowa State University, Ames, IA, 50011-1021.*
[c] *Department of Materials Science and Engineering, Iowa State University, Ames, IA, 50011-1096.*
†Electronic supplementary information (ESI) available. See DOI: 10.1039/x0xx00000

peaks of the starting materials nearly disappeared from the X-ray diffraction (XRD) patterns of the processed powder. *As-milled* powder was further analysed by XRD, Raman spectroscopy, high-angle annular dark-field scanning transmission electron microscopy (HAADF-STEM) and scanning transmission electron microscopy energy dispersive spectrometry (STEM-EDS). XRD and HAADF-STEM reveal structural disordering in the sample after 30 hours of milling, and indicate possibility of a uniform distribution of W and Mo atoms in the powder that might be associated with the formation of a solid solution-like material (Fig. 1a and Fig. S2, ESI†). However, the Raman spectrum of the sample (Fig. 1b) disagrees with that published for single-phase $(Mo_{1-x}W_x)S_2$.[11] On the contrary, it contains a set of broad peaks at 352, 380, 407 and 418 cm^{-1} that resemble those of the individual MoS_2 and WS_2 phases in laminar MoS_2/WS_2 heterostructures.[12] Annealing of a*s-milled* powder at 1000 °C for 16 hours in inert gas atmosphere produced a fused single-phase material, whose Raman spectrum matches that of single-phase $(Mo_{1-x}W_x)S_2$.[11] HAADF-STEM and STEM-EDS (Fig. S2, ESI†) also support the formation of the mixed compound. Unfortunately, MoS_2, WS_2 and $(Mo_{0.5}W_{0.5})S_2$ are nearly indistinguishable by XRD, which complicates the phase analysis of their mixtures and compounds. Therefore, to further explore the transformations of binary TMDCs, we studied an equimolar mixture of MoS_2 and WSe_2, whose XRD patterns are sufficiently different from one another to make the phase analysis by XRD conclusive (Fig. 2a). As in the previous case, equimolar quantities of MoS_2 and WSe_2 were mixed together and mechanically processed in the planetary mill at 600 rpm. Then, the obtained powder was heat treated at 1000 °C for 16 hours. The powder obtained after ball-milling and subsequent heat treatment is a single-phase $(Mo_{0.5}W_{0.5})SSe$, as illustrated in Fig. 2a. The Rietveld refinement results for this and other materials described in this work are listed in Table 1 and S1, ESI†. Given the different the X-ray scattering factors of Mo, W, Nb, Ta, S and Se, low Rietveld residuals shown in the table confirm statistical distribution of the scattering atoms on the corresponding crystallographic sites.[13] Also, the lattice parameters of $(Mo_{0.5}W_{0.5})SSe$ prepared in this work agree with those reported for a similar material synthesized from the elements.[14] The Raman spectrum of the heat treated TMDC further confirms the XRD results (Fig. 2b). It consists of three characteristic broad bands at about 265, 355 and 400 cm^{-1}, clearly deviating from those observed in the starting MoS_2, WSe_2 and *as-milled* sample. The XRD pattern of the latter indicates the presence of both MoS_2 and WSe_2 phases in the material even after 30 hours of ball-milling (Fig. S3a, ESI†). The XRD and Raman spectroscopy derived conclusion about makeup of the *fused* sample is further supported by high-resolution X-ray photoelectron spectroscopy (XPS), revealing the presence of all four principal elements, i.e. Mo, W, S and Se, on the surface of this material (Fig. S3b, ESI†), and STEM-EDS (Fig. S4, ESI†). In addition, the STEM-EDS investigation of the fused $(Mo_{0.5}W_{0.5})SSe$ that has been partially exfoliated by sonication in iso-propanol (Fig. 3) suggests random distribution of constituents within and between its layers.

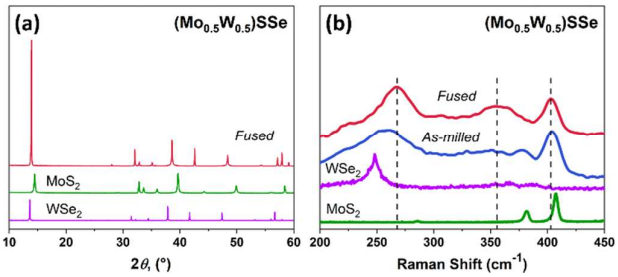

Fig. 2 $(Mo_{0.5}W_{0.5})SSe$. (a) XRD patterns and (b) Raman spectra of *as-milled* and milled then fused equimolar mixtures of MoS_2 and WSe_2. XRD patterns and Raman spectra of the starting materials are shown as references.

Since single-phase TMDCs consisting of more than four principal elements were unknown prior to this work, we explored the applicability of our synthetic approach to the preparation of five- and six-element materials (Table 1). Starting from bulk MoS_2, WSe_2 and $NbSe_2$, we synthesized a five-principal element compound with the nominal composition of $(Mo_{0.4}W_{0.2}Nb_{0.4})S_{0.8}Se_{1.2}$ (Fig. S5a, ESI†). Similar to the already discussed cases, after ball-milling, the material emerges as a highly disordered multi-phase composite. Its Raman spectrum (Fig. S5b, ESI†) contains two prominent peaks at 378 and 404 cm^{-1}, matching MoS_2, and a broad signal at ~245 cm^{-1} that combines characteristic peaks of $NbSe_2$ and WSe_2 at 228, 236, 248cm^{-1}. Annealing at 1000 °C converts *as-milled* powder into $(Mo_{0.4}W_{0.2}Nb_{0.4})S_{0.8}Se_{1.2}$ (Fig. S6, ESI†).

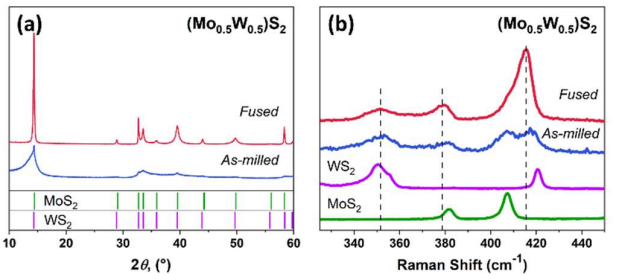

Fig. 1 $(Mo_{0.5}W_{0.5})S_2$. (a) XRD patterns and (b) Raman spectra of *as-milled* and milled then fused equimolar mixtures of MoS_2 and WS_2. Vertical bars in (a) indicate the Bragg peak positions of starting materials. Chart (b) also shows the Raman spectra of MoS_2 and WS_2.

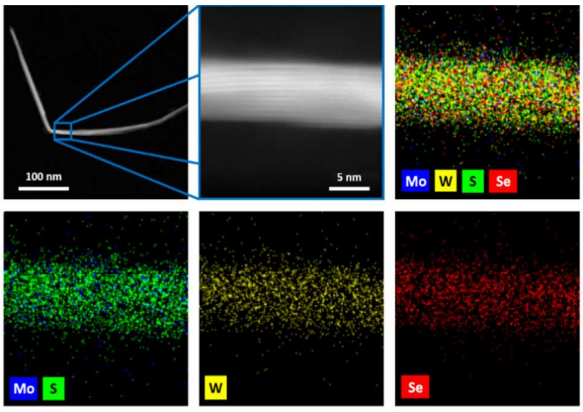

Fig. 3 HAADF-STEM and STEM-EDS images of the partially exfoliated single-phase $(Mo_{0.5}W_{0.5})SSe$. Due to X-ray signal overlap, Mo and S are shown together.

Table 1 Structural parameters of TMDCs derived from Rietveld refinements. The space group is P63/mmc (#194). Metal atoms (Mo, W, Nb or Ta) occupy 2c (1/3, 2/3, 1/4) site and chalcogens occupy 4f (1/3, 2/3, z) site. Standard deviations are given in parentheses.

	Lattice parameters			
Phase Composition	a, Å	c, Å	Chalcogen z/c	R_p[a]
$Mo_{0.5}W_{0.5}S_2$	3.1628(1)	12.3581(4)	0.6229(2)	6.77
$Mo_{0.5}W_{0.5}SSe$	3.2239(5)	12.7348(3)	0.6169(2)	6.99
$Mo_{0.4}W_{0.2}Nb_{0.4}S_{0.8}Se_{1.2}$	3.3073(2)	12.5718(9)	0.6151(2)	8.86
$Mo_{0.6}W_{0.2}Ta_{0.2}S_{0.8}Se_{1.2}$	3.1754(1)	12.4158(2)	0.6186(3)	9.01
$Mo_{0.25}W_{0.25}Nb_{0.25}Ta_{0.25}SSe$	3.3015(2)	12.5189(9)	0.6223(3)	8.82

[a] Column labelled R_p lists profile residuals.

Further, we also prepared $(Mo_{0.6}W_{0.2}Ta_{0.2})S_{0.8}Se_{1.2}$ (Table 1 and Figs. S5c,d, ESI†) from a stoichiometric mixture of $MoSe_2$, WS_2 and TaS_2 using the same procedure. In this instance, an extended annealing time of 72 hours was necessary to obtain a crystalline sample suitable for Rietveld refinement. Finally, the six-principal element compound, $(Mo_{0.25}W_{0.25}Nb_{0.25}Ta_{0.25})SSe$ (Table 1 and Figs. S5e,f, ESI†) has been made by ball-milling and subsequent thermal fusion of an equimolar (1:1:1:1) MoS_2, WSe_2, $NbSe_2$ and TaS_2 mixture. Extended annealing times required for the preparation of single-phase TMDCs conaining group 5 and 6 elements can be attributed to different stabilities and chemical reactivities of binary dichalcogenides, and may need to be adjusted for specific material's compositions

The XRD analysis reveals that the Bragg peaks in the diffraction patterns of all five- and six-principal element TMDCs remain substantially broadened even after a prolonged annealing, and a minor oxide impurity was detected only in the Ta-containing samples. Reasonably assuming similarity of the particle sizes and shapes in all three materials prepared from similar precursors, the observed Bragg peak broadening can be attributed to reduced crystallinity due to built-in strain. Since both Nb and Ta are larger than Mo and W, combining them in the same structure (layer) of a multi-element TMDC should cause distinct distortion of the layers that propagates into the 3D-lattice – the phenomenon known for high-entropy systems.[9]

The transformations enabling the formation of multi-element TMDCs from binary precursors can be understood if intrinsic properties of layered MX_2 materials are considered. It has been shown that due to the weakness of the vdW interactions, individual layers in TMDCs can slide against each other under external tangential forces[15] – the phenomenon responsible for the lubricating behaviours of layered metal dichalcogenides and their ability to exfoliate.[16] As a result, the tangential component of ball-milling[10b] enables mechanical exfoliation of bulk TMDCs.[17] At the same time, the exfoliated materials can restore their 3D-structures by restacking.[4] Hence, it is quite feasible that mechanical exfoliation and spontaneous restacking of different MX_2 layers, in a way similar to reshuffling a deck of playing cards, produces 3D hetero-assemblies. The experiments using low-speed (300 rpm) ball-milling of bulk MoS_2 and WSe_2 shed light upon this hypothesis. Contrary to the more intense (600 rpm) processing, both MoS_2 and WSe_2 phases remain clearly distinguishable in the XRD patterns of the *as-milled* powders even after 30 hours of milling at 300 rpm (Fig. S7, ESI†), and the STEM-EDS analysis now clearly reveals the presence of two different types of particles in the *as-milled* material (Fig. S8, ESI†). The first kind of particles looks compositionally uniform resembling particles in the *as-milled* samples discussed above. The second group of the particles consists of hetero-assemblies, where "reshuffling" remains incomplete, and individual MoS_2 and WSe_2 segments can be clearly distinguished. The Focused Ion Beam (FIB) cross-sectioning experiment performed on a large particle, which was cut by a Ga-ion beam, attached to a tungsten needle and rotated in the TEM chamber to produce a side view, unambiguously demonstrates its heterogeneous layered structure (Fig. 4), thus directly confirming our hypothesis. Annealing of the *as-milled* powder at 1000 °C for 16 hours produces a fused single-phase $(Mo_{0.5}W_{0.5})SSe$, which is identical to the materials obtained in other experiments (Fig. S9, ESI†). Thus, available experimental data strongly suggest that mechanical milling of MoS_2 with WSe_2 leads to a stochastic rearrangement of both individual layers and incompletely exfoliated slabs into 3D hetero-assemblies where building blocks retain their original compositional individuality (Fig. 4). Apparently, the energy of ball-milling is insufficient for their alloying and chemical reactions within such hetero-assemblies requires an additional energy input.

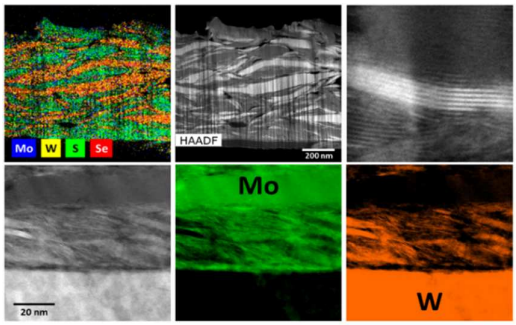

Fig. 4 HAADF-STEM and STEM-EDS images of the *as-milled* equimolar mixture of MoS_2 and WSe_2. Due to the higher Z-factor, WSe_2 fragments produce brighter image than the MoS_2 layers.

At ambient pressure, bulk MoS_2, WS_2 and WSe_2 are fairly stable up to ~1100 °C (Fig. S10, ESI†), but they slowly release chalcogens between 800–1000 °C in vacuum.[18] This suggests that all three binary TMDCs are approaching the edge of their stability at about ~1000 °C, where mobile reactive $\{MX_Y\}$ species formed can drive the chemical conversion of the 3D hetero-assemblies, generated during ball-milling, into single-phase multi-principal element TMDCs. At the same time, heating to lower temperatures, e.g. 500–800 °C, does not result in the fusion of such 3D hetero-assemblies. Remarkably, the multi-principal element TMDCs examined here retain their integrity even when high temperature heat treatment is extended to several weeks, and only trace amounts of metallic tungsten could be detected by XRD in *some* of the long-annealed samples, indicating remarkable stability of the multi-principal element TMDCs, which is characteristic of high-entropy systems.[9] Likely scenario, explaining the formation of

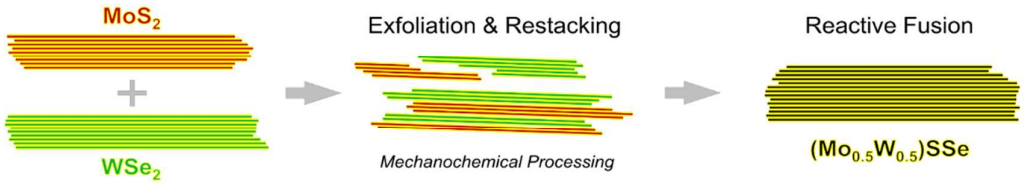

Fig. 5 Schematic diagram explaining formation of multi-principal element TMDCs via intermediate generation of stochastic 3-D nanostructures (middle) that coalesce into single-phase materials (right) during reactive (thermal) fusion. An equimolar physical mixture of MoS_2 and WSe_2 serves as illustrative example.

single-phase multi-principal element TMDCs from bulk precursors, can be imagined as a chain of physical and chemical events involving (i) mechanochemical exfoliation accompanied by (ii) reciprocal restacking of TMDC precursors, and (iii) reactive fusion of the resulting 3D hetero-assemblies as shown in Fig. 5 for the MoS_2-WSe_2 system. This reaction mechanism can also explain the earlier failure to obtain $(Mo_{0.5}W_{0.5})S_2$ from bulk MoS_2 and WS_2 via conventional alloying[6] where the reactive $\{MoS_x\}$ and $\{WS_y\}$ species must diffuse across much long distances.

In conclusion, the described synthetic approach enables easy and reliable preparation of diverse multi-principal element TMDCs that were either unknown or barely accessible via conventional materials fabrication routes. Mechanochemical exfoliation coupled with stochastic restacking of binary precursors into 3D hetero-assemblies, and reactive fusion of the latter into single-phase multi-element materials, represent critical steps in this novel approach. Another important outcome of this study is a proof that mechanochemical treatment facilitates the formation of 3D-heterostructures from binary TMDCs – an unexplored synthetic concept that may open doors to a broad range of unusual heterostructured nanomaterials. Finally, the developed synthetic technique expands our basic knowledge about chemical and physical transformations in metal-chalcogen systems under different types of processing and enables simple and reliable access to novel compositionally diverse materials unknown before.

This work was performed under auspices of the laboratory directed research and development (2018 LDRD) program. Ames Laboratory is operated for the U.S. Department of Energy by Iowa State University of Science and Technology under Contract No. DE-AC02-07CH11358. We thank Dr. Sergey Shilov from Bruker Optics, Bruker Corporation and Dr. Tao Ma from Ames Laboratory's Sensitive Instrument Facility for assistance.

Conflicts of interest

There are no conflicts to declare.

Notes and references

1 (*a*) A. Kolobov and J. Tominaga. *Springer Series in Materials Science, 239. Two-Dimensional Transition-Metal Dichalcogenides;* Springer International Publishing AG: Switzerland, 2016; (*b*) *Semiconductors and Semimetals. v. 95, 2D Materials*; F. Lacopi, J. J. Boeckl, and C. Jagadish, Eds.; Academic Press: Cambridge, San Diego, Oxford, London, 2016.

2 J. R. Brent, N. Savjani, and P. O'Brien *Prog. Mater. Sci.* 2017, **89**, 411–478.

3 S. Susarla, A. Kutana, J. A. Hachtel, V. Kochat, A. Apte, R. Vajtai, J. C. Idrobo, B. I. Yakobson, C. S. Tiwary, and P. M. Ajayan, *Adv. Mater.* 2017, **29**, 1702457.

4 (*a*) A. K. Geim and I. V. Grigorieva, *Nature* 2013, **499**, 419–425; (*b*) K. S. Novoselov, A. Mishchenko, A. Carvalho, and A. H. Castro, Neto *Science* 2016, **353**, aac9439.

5 (*a*) X. Chia, A. Y. S. Eng, A. Ambrosi, S. M. Tan and M. Pumera, *Chem. Rev.* 2015, **115**, 11941–11966; (*b*) J. Li, X. Shi, J. Fang, J. Li, and Z. Zhang, *ChemNanoMat* 2016, **2**, 997–1002; (*c*) D. Wang, Z. Wang, C. Wang, P. Zhou, Z. Wu and Z. Liu, *Electrochem. Commun.* 2013, **34**, 219–222; (*d*) K. Krishnamoorthy, P. Pazhamalai, G. Veerasubramani and S. J. Kim, *J. Power Sources* 2016, **321**, 112–119; (*e*) Y. Dai, X. Wu, D. Sha, M. Chen, H. Zou, J. Ren, J. Wang and X. Yan, *Electron. Mater. Lett.* 2016, **12**, 789–794.

6 C. Thomazeau, C. Geantet, M. Lacroix, V. Harlé, S. Benazeth, C. Marhic and M. Danot, *J. Solid State Chem.* 2001, **160**, 147–155.

7 (*a*) W. Choi, N. Choudhary, G.H. Han, J. Park, D. Akinwande, and Y. H. Lee, *Mater. Today* 2017, **20**, 116–130; (*b*) N. Choudhary, J. Park, J. Y. Hwang, H.-S. Chung, K. H. Dumas, S. I. Khondaker, W. Choi and Y. Jung, *Sci. Rep.* 2016, **6**, 25456;(*c*) S. Zheng, L. Sun, T. Yin, A. M. Dubrovkin, F. Liu, Z. Liu, Z. X. Shen and H. J. Fan, *Appl. Phys. Lett.* 2015, **106**, 063113; (*d*) Y. Kobayashi, S. Mori, Y. Maniwa and Y. Miyata, *Nano Res.* 2015, **8**, 3261–3271; (e) J. Shi, R. Tong, X. Zhou, Y. Gong, Z. Zhang, Q. Ji, Y. Zhang, Q. Fang, L. Gu, X. Wang and Z. Liu, *Adv. Mater.* 2016, **28**, 10664–10672.

8 (*a*) Y. Lei, S. Pakhira, K. Fujisawa, X. Wang, O. O. Iyiola, N. Perea López, A. Laura Elías, L. Pulickal Rajukumar, C. Zhou, B. Kabius and N. Alem, *ACS Nano* 2017, **11**, 5103–5112; (*b*) L. Wang, Z. Sofer, J. Luxa, M. Pumera, *Adv. Mater. Interfaces* 2015, **2**, 1500041; (*c*) K. Chen, X. Wan, W. Xie, J. Wen, Z. Kang, X. Zeng, H. Chen and J. Xu, *Adv. Mater.* 2015, **27**, 6431–6437.

9 D. B. Miracle and O. N. Senkov, *Acta Mater.*2017, **122**, 448–511.

10 (*a*) V. Balema, V. Pecharsky and K. Dennis, *J. Alloys Compd.* 2000, **313**, 69–74; (*b*) C. Suryanarayana, *Prog. Mater. Sci.* 2001, **46**, 1–184.

11 D. O. Dumcenco, K. Y. Chen, Y. P. Wang, Y. S. Huang and K. K. Tiong, *J. Alloys Compd.* 2010, **506**, 940–943.

12 C.-R.Wu,X.-R. Chang, T.-W. Chu, H.-A. Chen, C.-H. Wu and S.-Y. Lin, *Nano Lett.* 2016, **16**, 7093–7097.

13 V.K. Pecharsky and P. Zavalij. *Fundamentals of Powder Diffraction and Structural Characterization of Materials* 2nd Ed. Springer-Verlag US: New York, 2009.

14 D. Palit, S. K. Srivastsva and M. C. Chakravort, *J. Mat. Sci. Lett.* 1996, **15,** 1115–1118.

15 J. P. Oviedo, S. KC, N. Lu, J. Wang, K. Cho, R. M. Wallace, M. J. Kim, *ACS Nano* 2015, **9**, 1543–1551.

16 J. Kang, V. K. Sangwan, J. D. Wood, and M. C. Hersam, *Acc. Chem. Res.* 2017, **50**, 943–951.

17 (*a*) M. Kostecki and E. Jezierska, *Nanomat. Nanotech.* 2014, **4**, 1–9; (*b*) Q. H. Wang, K. Kalantar-Zadeh, A. Kis, J. N. Coleman and M. S. Strano, *Nat. Nanotechnol.* 2012, **7**, 699–712.
18 (*a*) A. Azizi, S. Eichfeld, G. Geschwind, K. Zhang, B. Jiang, D. Mukherjee, L. Hossain, A. F. Piasecki, B. Kabius, J. A. Robinson and N. Alem, *ACS Nano* 2015, **9**, 4882–4890; (*b*) W. A. Brainard, *NASA Tech. Note D-5141* 1968, 1–26.